TRANSVERSE IMPEDANCE DISTRIBUTION MEASUREMENTS USING THE RESPONSE MATRIX FIT METHOD AT APS*

V. Sajaev, Argonne National Laboratory, Argonne, IL 60439 USA

Abstract

The Advanced Photon Source storage ring has a number of narrow-gap insertion device vacuum chambers, and there is a plan to further increase their number. These vacuum chambers contribute to the impedance of the machine and to the impedance limits the single-bunch current threshold. In order to understand the contribution of the vacuum chambers and its dependence on the gap, the distribution of the vertical transverse impedance around the circumference of the APS storage ring has been determined using the response matrix fit method. This method allows us to find focusing errors around the storage ring and was originally used to determine and correct the linear model of the APS. The high accuracy of the method enables us to measure the variation of betatron phase advance around the ring with beam current. Results of these measurements are reported and the impedance of different parts of the storage ring is presented.

INTRODUCTION

The Advanced Photon Source (APS) is a third-generation synchrotron light source based on a 7-GeV electron storage ring. The synchrotron radiation is mainly produced by undulators. Optimization of beamlines calls for small undulator gaps. Therefore the undulators are installed on dedicated small gap insertion device (ID) vacuum chambers. APS has 35 5-m-long straight sections available for undulators; 27 of them are currently occupied. Most of the ID vacuum chambers have an 8-mm inner aperture, and two chambers have a 5-mm aperture. These vacuum chambers are believed to be the main source of the transverse impedance of the machine.

Our goal is to measure the vertical transverse impedance distribution around the machine and determine the contribution of the ID vacuum chambers. Although one can measure the combined effects of all chambers by measuring the transverse tune shift with single-bunch current [1], it is difficult to accurately measure the small change in this tune shift after only one or a few new ID chambers are installed.

In the past a number of attempts have been made to measure the impedance of separate parts of accelerators. Phase advance measurements from beam position monitor (BPM) turn-by-turn histories were used at LEP [2] to measure the impedance distribution around the ring. This method was tried at APS; however, the accuracy of the measurements was not sufficient to determine the impedance of a single ID vacuum chamber. Recently, the accuracy of turn-by-turn BPM measurements at APS was greatly improved using the Model Independent Analysis (MIA) [3]. It was demonstrated that with MIA the phase advance measurements similar to LEP provide enough accuracy to reveal the main impedance structure of the APS ring. However, this work was not pursued. There is also a different approach, which uses local orbit bumps to probe different parts of an accelerator [4-6]. All these methods employ the fact that the beam sees the impedance as a defocusing quadrupole whose strength depends on the beam current.

At APS we have implemented a method for precise measurement of beta functions along the ring [7]. The method employs an orbit response matrix fit to determine the distribution of focusing errors around the machine and then uses these errors to calculate beta functions (the details on the response matrix fit and more references can be found in [8]). Since the impedance can be represented as a current-dependent quadrupole, the measurement of the beta functions with different currents could be used to determine the impedance distribution around the machine.

We report on a sensitive method for measuring the transverse impedance distribution along the machine that uses the response matrix fit method to calculate local betatron phase advance changes due to different beam currents.

RESPONSE MATRIX FIT

The orbit response matrix is the change in the orbit at the BPMs as a function of the changes in steering magnets. The response matrix is defined by the linear lattice of the machine; therefore it can be used to calibrate the linear optics in a storage ring.

The main idea of the analysis is to adjust the quadrupole gradients of a computer model of the storage ring until the model response matrix best fits the measured response matrix. The problem of fitting the response matrix is solved in the following way. Let the response matrix M be a function of the vector of variables x. Then we need to solve the equation

$$M_{measured} - M_{model}(x) = 0$$

which can be solved by Newton's method:

$$\Delta x = \left(\frac{\partial M_{model}}{\partial x} \right)^{-1} \cdot \left(M_{measured} - M_{model}(x_0) \right),$$

where x_0 corresponds to the initial model. To solve this equation, we rewrite the response matrix as one vector consisting of $N_{corr} \times N_{bpm}$ values, where N_{corr} is the number of correctors used in the response matrix and N_{bpm} is the number of BPMs. Then the derivative of the response matrix would be a $(N_{corr} \times N_{bpm}) \times N_{var}$ matrix, where N_{var} is the number of variables upon which the response matrix depends. Finally, to fit the response matrix, we have to determine all variables upon which the response matrix depends, calculate the derivative of the response matrix

* This work is supported by U.S. Department of Energy, Office of Basic Energy Sciences under Contract No. W-31-109-ENG-38.

with respect to these variables, and then invert it. After that, the solution can be found by iteration.

The most obvious and important variables are focusing errors (quadrupole calibration errors or orbit errors in sextupoles), corrector calibration errors, and BPM gain errors. Another obvious but less important variable is the energy shift associated with the changing of each steering magnet. The choice of what variables to use depends on details of the particular storage ring and how accurately the response matrix can be measured.

The APS storage ring is 40-fold periodic. Each sector consists of two dipoles, ten quadrupoles, and seven sextupoles. There are also eight horizontal and eight vertical steering magnets and nine to eleven BPMs per sector. Possible focusing errors could come from miscalibration of quadrupole power supplies (each quadrupole at APS has its own power supply) and from horizontal orbit errors in sextupoles, so that the total possible number of focusing errors per sector could be up to 17. Obviously, there are not enough BPMs to resolve all possible focusing errors; therefore we keep only quadrupoles in our model. Since the average betatron phase advance per quadrupole is only 0.09, we consider that the quadrupoles alone could accurately reproduce all possible focusing errors in the storage ring.

In order to limit the size of the derivative of the response matrix, we use only 40 horizontal and 40 vertical correctors and all available BPMs. In this case the two-dimensional uncoupled response matrix contains about 32,000 elements and depends on approximately 1400 variables. The overall size of the derivative in double precision is about 350 MB.

MEASUREMENTS

The APS storage ring vacuum chambers are made of aluminum and have an elliptic 85×42 mm size. When an undulator is installed in a sector, a 5-m-long section of the vacuum chamber is replaced with a narrow-gap ID chamber (total length of one sector is 27.6 m). Most of the APS insertion devices have 8-mm-gap vacuum chambers; two IDs in sectors 3 and 4 have 5-mm-gap vacuum chambers. Normal and ID vacuum chambers are connected with 20-cm-long tapers. Figure 1 represents locations of the small-gap vacuum chambers installed at the APS storage ring at this moment. We expect the vertical impedance to be dominated by these small-gap ID vacuum chambers.

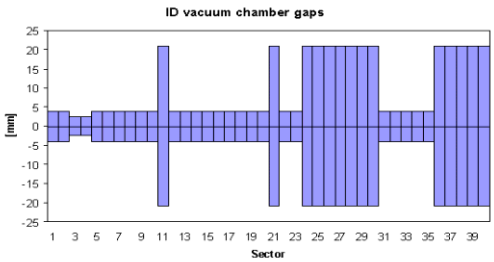

Figure 1: ID vacuum chamber gaps.

In order to obtain the change in focusing around the ring with the beam intensity, we measure the response matrices for different beam currents, analyze them to get beta functions, and then compare the local phase advances. Figure 2 shows the phase advance difference between the two response matrices measured with 10 mA and 1 mA in a single bunch. One can easily see a sharp change in phase caused by 5-mm chambers in sectors 3 and 4 and flat regions corresponding to no ID chambers in sectors 24 to 30 and 36 to 40. Fast oscillation of the phase advance difference is explained by beta function mismatch, caused by changes in focusing. Figure 2 confirms our expectations that the main contribution comes from ID vacuum chambers.

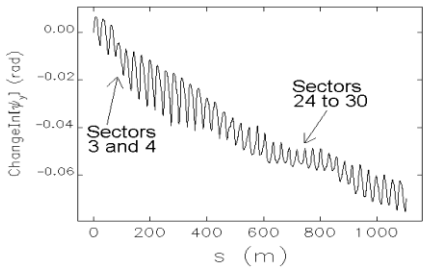

Figure 2: Betatron phase advance difference between 10-mA and 1-mA cases.

This measurement also yields the tune slope with current, which can be used to calculate the total transverse impedance. Figure 3 (left) shows vertical betatron tune dependence on the beam current defined by the following formula:

$$\frac{d\nu}{dI} = \frac{R}{2\pi\sigma_s E}\sum\langle\beta\rangle_i Z_{eff}^{(i)} .$$

The measurements are so accurate that one can see a deviation from linear dependence due to bunch length variation with the current. To keep the bunch length constant, the rf voltage was varied during measurements.

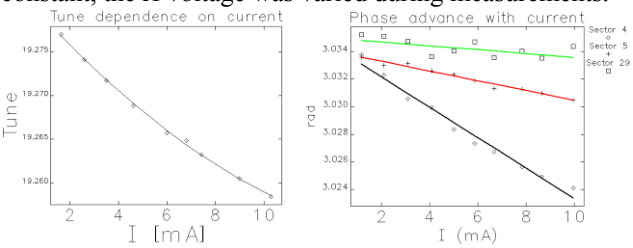

Figure 3: Left – vertical tune slope with current. Right – vertical phase advance slopes with current for different sectors.

In order to get the local distribution of the impedance around the ring, we analyze the phase-advance changes due to a change in the beam current sector by sector. Figure 3 (right) shows typical betatron phase-advance slopes for sectors 4, 5, and 29 (5-mm-, 8-mm- and 42-mm-gap ID vacuum chambers, respectively).

The APS storage ring operates in two different modes: 7.7-nm high-emittance lattice and 2.4-nm low-emittance lattice. The vertical beta functions of the two lattices are almost equal in the locations of the ID vacuum chambers, but have different average vertical beta functions. Phase

slope distribution measurements were conducted for both low-emittance and high-emittance lattices. Though the transverse impedance does not change with the lattice, the defocusing effect of the impedance depends on beta functions; therefore the phase-advance slope is expected to be similar for sectors with small-gap vacuum chambers. Figure 4 presents the distribution of phase slope with current along the APS storage ring for two lattices. As expected, the biggest phase advance change occurs in sectors 3 and 4, where 5-mm vacuum chambers are installed. Also, all sectors without small-gap chambers are clearly seen. It is important to note that the phase-advance changes for sectors 24 through 30 are larger for the low-emittance lattice. This is explained by the fact that for these sectors the impedance is approximately evenly distributed along the sector, and the scaling is due to average vertical beta function difference. Thus the measurements are reliable even for sectors without the small-gap ID vacuum chambers.

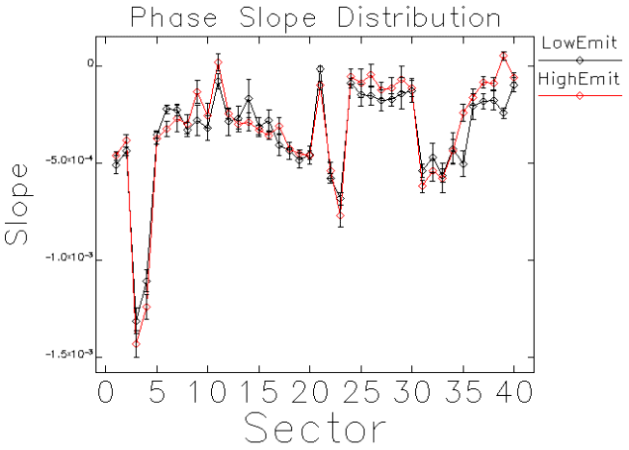

Figure 4: Phase advance slopes distribution.

The effective transverse impedance is the integral over the machine impedance, multiplied by the bunch spectrum squared. For a particular impedance component, it can be found from measured slopes of the phase advance

$$Z_{eff}^{i} = \frac{E\sigma_s}{R\beta_i}\frac{d\mu}{dI}.$$

The beta functions have to be taken at the location of the impedance elements. For the ID vacuum chamber we use the average over the 5-m-long ID straight section, otherwise we use the beta function averaged over the entire sector. The bunch length is 40 ps and is maintained approximately constant during measurements by varying the rf voltage. The resulting values for the various sectors as well as the total effective vertical impedances are shown in Table 1 for both high- and low-emittance lattices. The phase-advance slopes and impedances shown in the table are averaged over all similar sectors, i.e., all empty sectors, all sectors with 8-mm ID vacuum chambers, etc. For calculation of the impedance of the ID vacuum chambers Z_{8mm}^{eff} and Z_{5mm}^{eff}, the average phase slope of the empty sector was subtracted. These results compare well with the impedance model and with the measurements in [5].

Table 1: Phase Slopes and Impedances

		High Emittance	Low Emittance
$\langle\beta\rangle_{sector}$	m	12.2	16.3
$\langle\beta\rangle_{ID}$	m	4.7	3.7
$d\mu/dI_{no\ ID}$	rad/A	-0.09	-0.14
$d\mu/dI_{8mm}$	rad/A	-0.39	-0.40
$d\mu/dI_{5mm}$	rad/A	-1.33	-1.21
Z_{noID}^{eff}	kΩ/m	3.5	4.1
Z_{8mm}^{eff}	kΩ/m	31	34
Z_{5mm}^{eff}	kΩ/m	126	138
Z_{total}^{eff}	MΩ/m	1.06	1.17

CONCLUSION

Analysis of the measured orbit response matrix provides detailed information concerning storage ring optics. The optics measurements are so precise that one can see the phase-advance difference due to different beam currents. This was used to derive the distribution of the vertical impedance around the APS storage ring. It was found that the small-gap ID vacuum chambers contribute the most to the storage ring vertical impedance. The actual values of the vertical impedance of the chambers with different gaps were determined.

ACKNOWLEDGMENTS

The author would like to thank the staff at the APS, particularly Steve Milton for his encouragement and support of the work and Louis Emery for tremendous help with operational, software, and physics issues. Also, the author would like to thank K. Harkay, Y.-C. Chae, and E. Trakhtenberg for numerous useful discussions and H. Shang for helping with programming.

REFERENCES

[1] K. Harkay and N. Sereno, Proceedings of PAC 1997, Vancouver, Canada, p. 1700 (1998).
[2] D. Brandt et al, Proceedings of PAC 1995, Dallas, p. 570 (1996).
[3] C.-X. Wang, Proceedings of PAC 2001, Chicago, p. 1354 (2001).
[4] V. Kiselev, V. Smaluk, "A Method for Measurement of Transverse Impedance along Storage Ring," Proceedings of the 4th European Workshop on Diagnostics for Particle Accelerators, Chester, 1999.
[5] L. Emery, G. Decker and J. Galayda, Proceedings of PAC 2001, Chicago, p.1823 (2001).
[6] L. Farvacque, E. Plouviez, Proceedings of EPAC 2002, Paris, p.1550 (2002).
[7] V. Sajaev, L. Emery, Proceedings of EPAC 2002, Paris, p. 742 (2002).
[8] J. Safranek, Nucl. Instrum. Methods A 388, p. 27 (1997).